

Stopband optimised *E*-plane filters with multiple metal inserts of variable number per coupling element

Prof. F. Arndt, Dr.-Ing., Sen.Mem.I.E.E.E., D. Heckmann, Dipl.-Ing., H. Semmerow, Dipl.-Ing., J. Bornemann, Dr.-Ing., and R. Vahldieck, Dr.-Ing., Mem.I.E.E.E.

Indexing term: Waveguides and waveguide components

Abstract: Improved stopband attenuation of *E*-plane filters is achieved by replacing merely a few of the conventional single insert coupling elements by triplets or quintuplets of metal inserts. The method of field expansion into suitable eigenmodes used considers the effects of finite insert thickness and the mutual higher order mode interaction of all inserts. Calculated stopband attenuations of more than 50 dB up to about 30 GHz, or 60 GHz, respectively, have been attained, although the passbands of the corresponding filter examples are chosen to operate at the upper waveguide band limit of the mount (at 18 GHz for Ku-band and at 40 GHz for Ka-band, respectively). The results demonstrate that high stopband conditions can be satisfied by designs with only a modified number of multiple inserts. This helps to maintain the low-loss and low-cost qualities of *E*-plane filters and also provides for improved stopband demands. The thickness of all inserts of $t = 190 \mu\text{m}$ makes possible accurate metal-etching fabrication.

1 Introduction

Metal inserts integrated in the *E*-plane of rectangular waveguides are common building blocks in low-cost low-loss millimetre-wave filter designs [1-4]. For filters with passbands within, approximately, the upper half of the fundamental mode band of the used waveguide mount, the attenuation in the upper stopband attainable with single inserts may, however, often be too low for many applications, e.g. for duplexers. This is due to increasing direct power transfer along the single strip sections [5] if the frequency exceeds the fundamental mode cutoff frequency of the coupling sections, which is determined by the distance between the strip and the waveguide sidewalls.

The problem has been attacked, more recently, by replacing all single strips within a filter by double- [5, 6] or triple-strip [7] sections. However, improved attenuation in the second stopband may already be attained if only a moderate number of the coupling sections still operate below cutoff frequency. Therefore, concerning low-loss and low-cost requirements, a variable instead of a constant number of metal inserts along the filter section (Fig. 1) is often considered to be a more convenient technical solution for *E*-plane filters with broad second stopbands.

Filters with single [8], double [9] and triple inductive round posts [10-13] have been presented in Reference 11. The rectangular strip structure of Fig. 1, however, has the advantage of being producible by an accurate metal-etching technique, which is appropriate for low-cost mass production and avoids the necessity for tuning devices.

Inductive strips have been analysed using the variational and the moment method [14-16]. The reflection at an *N*-furcated parallel-plate waveguide junction has been treated more recently [17]. However, the immediate higher order mode interaction between series connected strip elements of different numbers of strips, which is important to calculate the stopband behaviour of related filter structures, has not yet been analysed.

In this paper, therefore, the design of optimised *E*-plane

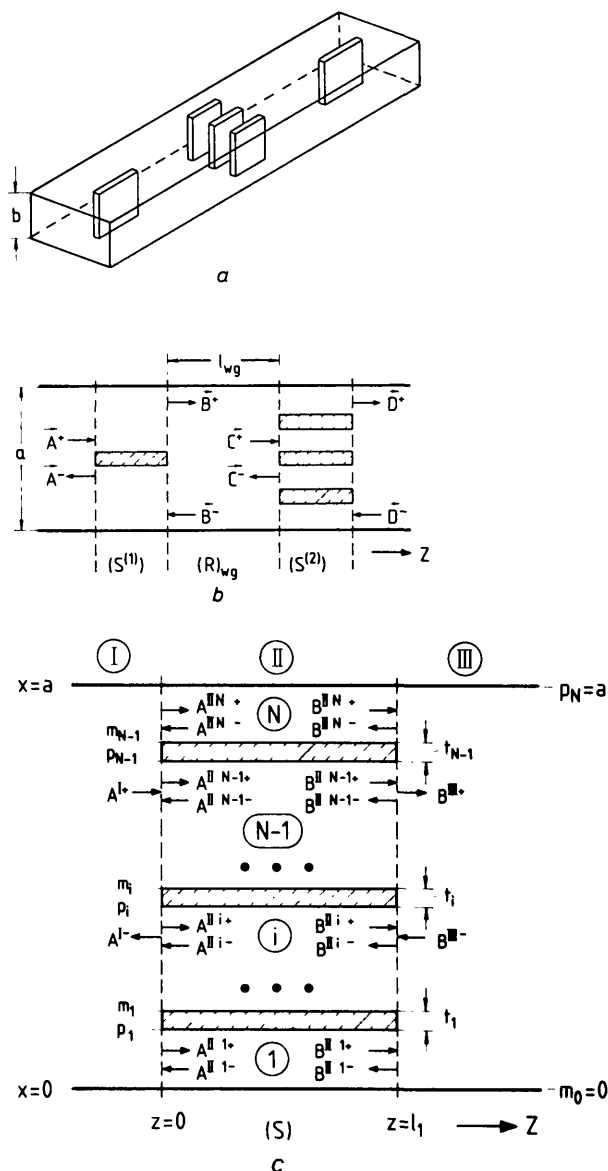


Fig. 1 *E*-plane filter with multiple metal inserts of variable number per coupling element

a Waveguide and inserts
b Coupling sections with variable number of inserts
c $(N - 1)$ strip section of finite length l_1

Paper 4571H (E12), received 28th November 1985

F. Arndt, D. Heckmann, H. Semmerow, and J. Bornemann are with the Microwave Department, University of Bremen, Kufsteiner Str., NW-1, D-2800 Bremen 33, W. Germany. R. Vahldieck is with the Department of Electrical Engineering, University of Ottawa, Ontario, Canada

integrated circuit filters with a variable number of $(N - 1)$ metal inserts (Fig. 1) is based on the rigorous field expansion [18, 19] into suitable incident and scattered waves at all discontinuities, beyond as well as below the cutoff frequencies. Matching the fields at the discontinuities yields the corresponding modal scattering matrices, which are directly combined with the intermediate waveguide sections to the overall matrix of the filter. An optimisation computer program varies the insert dimensions and filter resonator lengths until insertion loss and stopband attenuation meet given specifications.

2 Theory

The general coupling section (Fig. 1c) of the filter with variable number of inserts (Figs. 1a, b) is assumed to consist of $(N - 1)$ metal strips, i.e. of an N -furcated rectangular waveguide section, of length l_1 . For each corresponding subregion $v = I, III_1, III_2, \dots, III_i, \dots, III_N$ (Fig. 1c) the fields [18] at $z = 0$

$$\begin{aligned} E^{(v)} &= -j\omega\mu\nabla \times \mathbf{\Pi}_{hx}^{(v)} \\ H^{(v)} &= \nabla \times \nabla \times \mathbf{\Pi}_{hx}^{(v)} \end{aligned} \quad (1)$$

are derived from the x -component of the magnetic Hertzian vector potential $\mathbf{\Pi}_h$, which is assumed to be the sum of suitable eigenmodes [18–20] satisfying the Helmholtz equation and the boundary conditions at the metallic surfaces

$$\mathbf{\Pi}_{hx}^{(v)} = \mathbf{e}_x \cdot \sum_{m=1}^{\infty} T_m^{(v)} \sin \frac{m\pi}{p^{(v)}} f^{(v)} \cdot [A_m^{(v)+} - A_m^{(v)-}] \quad (2)$$

The still unknown eigenmode amplitude coefficients $A_m^{(v)\pm}$ of the forward and backward waves are suitably normalised [18] by $T_m^{(v)}$ to yield directly the corresponding scattering matrix. The abbreviations in eqn. 2 are elucidated in Appendix 6.

Matching the tangential field components at $z = 0$ (Fig. 1c) and utilising the orthogonality property of the related eigenfunctions [18, 19], yields the scattering matrix at $z = 0$. The same is true at $z = l_1$. For the corresponding relations, the reader is referred to Reference [20] (eqns. 5–7), where the number of subsections has to be increased to N , instead of 4.

The scattering matrix of the complete $(N - 1)$ metal strip section of length l_1 (Fig. 1c)

$$\begin{pmatrix} A^{I-} \\ B^{III+} \end{pmatrix} = \begin{pmatrix} (S_{11}) & (S_{12}) \\ (S_{21}) & (S_{22}) \end{pmatrix} \begin{pmatrix} A^{I+} \\ B^{III-} \end{pmatrix} \quad (3)$$

for completeness, is given in Appendix 6.

The series connection of several metal strip sections is calculated by directly combining the related scattering matrix elements [20]. This procedure leads to expressions containing only exponential functions with negative argument. So the otherwise known numerical instabilities due to resonance and interference effects of higher order modes below their cutoff frequencies may be avoided.

For the calculations in this paper, the expansion into fifteen eigenmodes at each discontinuity yields sufficient convergence of the scattering matrix coefficient. This is demonstrated in Fig. 2, where the magnitude of the scattering coefficient $|S_{21}|$ of the filter of Fig. 4a (dashed line) at $f = 20$ GHz is plotted against the number M of modes considered.

For the design of optimised E -plane filters with variable number of inserts an error function to be minimised is defined [20]. For given waveguide housing dimensions,

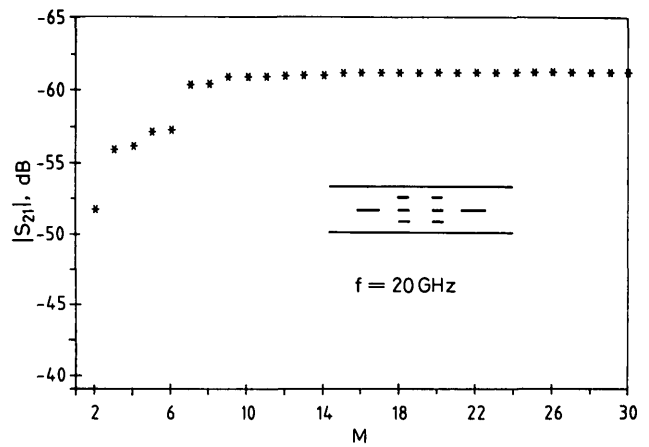


Fig. 2 Insertion loss in decibels as a function of subsequent modes M considered

For the filter example of Fig. 4a, dashed-line

thickness t , number $(N - 1)$ of the inserts, and number of the resonators, the parameters to be optimised are the metal insert and resonator lengths. Opposite to a lumped-element circuit-type approach, this computer optimisation takes into account higher order mode coupling effects. Therefore, the stopband attenuation behaviour of the filter can be included in the optimisation process.

3 Results

Figs. 3 show the improvement of the stopband behaviour for a Ku-band (12–18 GHz, Fig. 3a) and a Ka-band (26–40 GHz, Fig. 3b) two-resonator filter, for passbands at about half the waveguide band, if the second insert of the single metal insert filter is replaced by a triplet of inserts. The

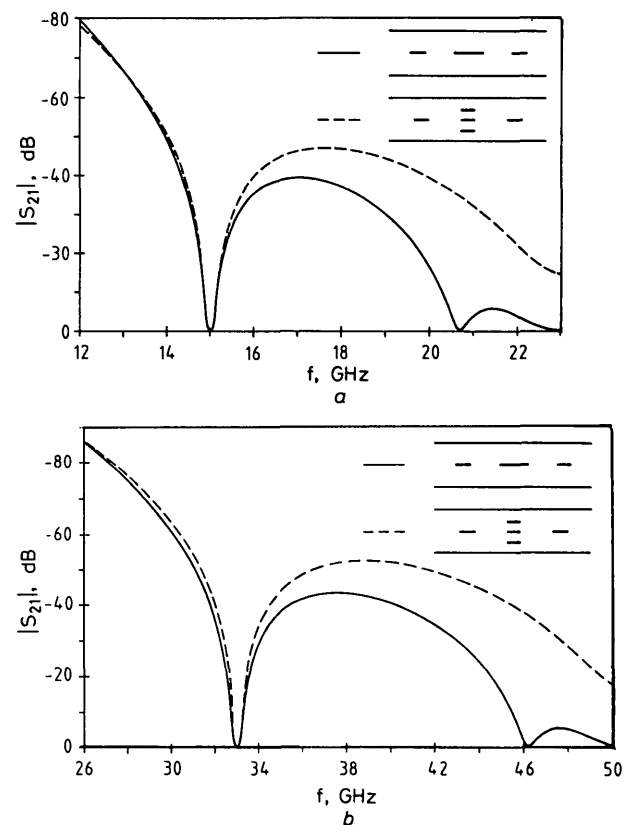


Fig. 3 Insertion loss as a function of frequency for two-resonator filters with single and triple metal inserts for the second coupling section

a Ku-band example
b Ka-band example
— single metal insert
--- triple metal insert

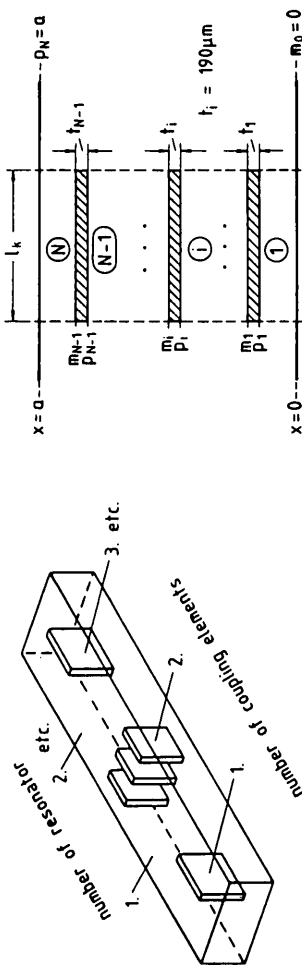


Table 1: Computer optimised design data for E-plane filters with variable number of inserts

Frequency band waveguide housing	Number of resonator	Length of resonator, mm	Number of coupling element	l_k	ρ_1	m_1	ρ_2	m_2	ρ_3	m_3	ρ_4	m_4	ρ_5	m_5	Figure
Ku — band (R 140) $a = 15.799$ mm $b = 7.899$ mm	1 and 2	8.840	1 and 3	4.818	7.804	7.994									3a
	1 and 2	10.081	1 and 3	11.931	7.804	7.994									3a
	1 and 3	8.832	1 and 4	2.985	4.277	4.467	7.804	7.994	11.331	11.521					4a
	2	8.790	2 and 3	9.800	7.804	7.994									4a
	1 and 3	6.540	1 and 4	24.535	7.804	7.994									4a
	2	8.006	2 and 3	8.229	7.804	7.994									4c
	1 and 3	6.754	1 and 4	4.053	3.597	3.787	7.804	7.994	12.011	12.201					5a
	2	8.417	2 and 3	7.899	7.804	7.994									5a
	1 and 4	8.840	1 and 5	2.663	2.585	2.775	4.251	4.441	7.804	7.994	11.357	11.547	13.023		5a
	2 and 3	8.840	2 and 4	11.931	7.804	7.994									5a
	1 and 4	8.996	1 and 5	12.931	7.804	7.994									5a
	2 and 3	9.942	2 and 4	1.924	7.804	7.994									5a
	1 and 4	6.622	1 and 5	9.066	7.804	7.994									5a
	2 and 3	8.080	2 and 4	3.802	3.244	3.434	7.804	7.994	12.364	12.554					5b
	1 and 3	9.964	1 and 4	6.245	7.804	7.994									5b
2	11.088	2 and 3	3.300	3.987	4.177	7.804	7.994	11.621	11.811					5b	
1 and 2	4.249	1 and 3	4.020	3.651	3.841	7.804	7.994	11.957	12.147					6a	
1 and 2	4.791	1 and 3	5.148	7.804	7.994									6b	
1 and 3	2.409	1 and 4	3.660	3.500	3.690	7.804	7.994	12.108	12.298					6b	
2	3.117	2 and 3	2.181	3.461	3.651									3b	
1 and 3	3.756	1 and 4	5.110	3.461	3.651									3b	
1 and 3	3.198	1 and 4	2.400	3.461	3.651									3b	
2	3.928	2 and 3	1.261	1.925	2.115	3.461	3.651	4.997	5.178					4b	
1 and 3	3.198	1 and 4	3.673	3.461	3.651									4b	
2	3.928	2 and 3	8.974	3.461	3.651									4b	
1 and 3	3.198	1 and 4	3.196	3.461	3.651									4b	
2	3.928	2 and 3	1.567	1.619	1.807	3.461	3.651	5.303	5.493					4b	
1 and 3	3.198	1 and 4	4.140	3.461	3.651									4b	
2	3.928	2 and 3	1.254	1.250	1.440	1.880	2.070	3.461	3.651	5.042	5.232	5.672	5.862	4b	

All dimensions in mm

inserts are each $190\ \mu\text{m}$ thick to make the metal etching manufacturing technique possible. The optimised design data are given in Table 1.

For filters with passbands at the upper limit of the corresponding fundamental mode waveguide band of the mount, the improvement of the stopband behaviour by replacing single metal inserts by multiple inserts is still more evident. This is demonstrated in Figs. 4, where the magnitude of $|S_{21}|$ in decibels of corresponding Ku-band (Figs. 4a and 4c) and Ka-band (Fig. 4b) three-resonator filters are plotted against frequency. Although the passband bandwidths of the filters are not identical, Fig. 4a shows clearly the amelioration of the stopband attenuation attainable by triple inserts. The ultra-broad second stopband, which can be achieved by multiple inserts for the

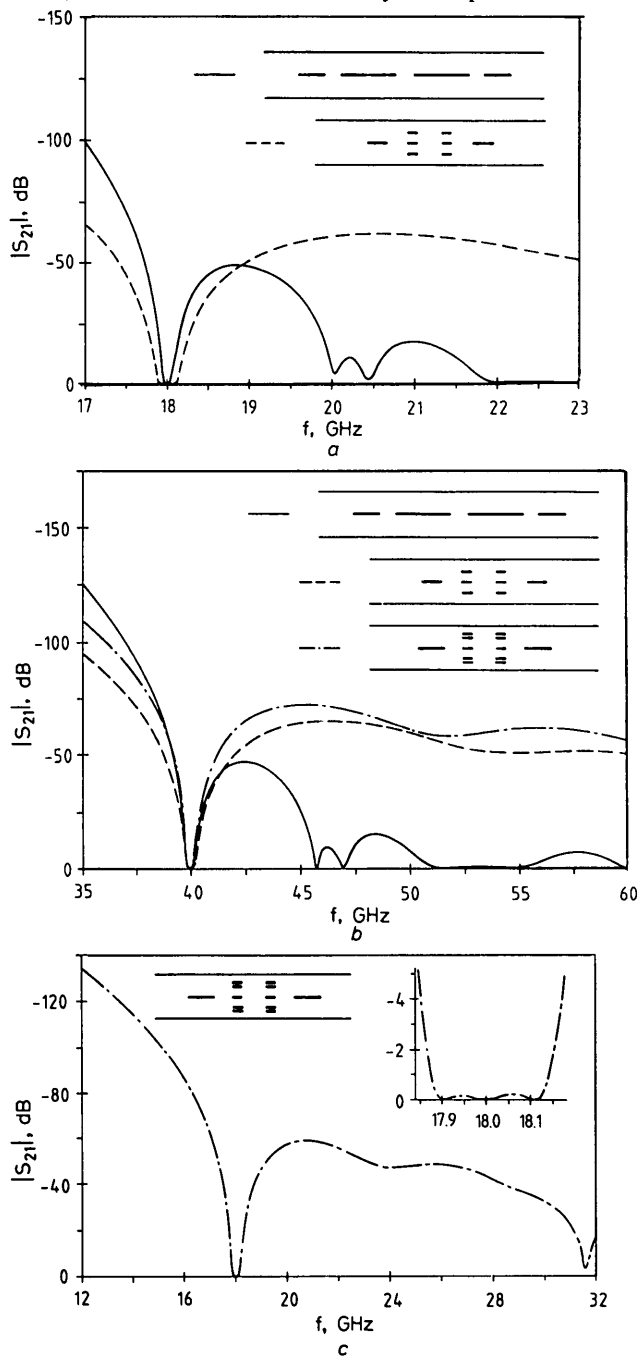


Fig. 4 Insertion loss as a function of frequency for three-resonator filters with single, triple and quintuple metal inserts for the second and third coupling section
a Ku-band example with single and triple inserts
b Ka-band example
c Ku-band example with quintuple inserts
 — single metal insert
 - - - triple metal insert
 - · - quintuple metal insert

inner coupling sections, instead of single inserts, is illustrated of the examples of Figs. 4b and 4c, where the filters have nearly identical passband bandwidths. Although the mode suppression properties of a triplet of inserts are already excellent [10–16], still improved stopband characteristic is possible by fivefold inserts.

For four-resonator filters, either only the central coupling section (Fig. 5a) or the three inner coupling sections (Fig. 5b) may be replaced by a multiple strip section. Better stopband behaviour, however, is achieved by the three triplets (Fig. 5b).

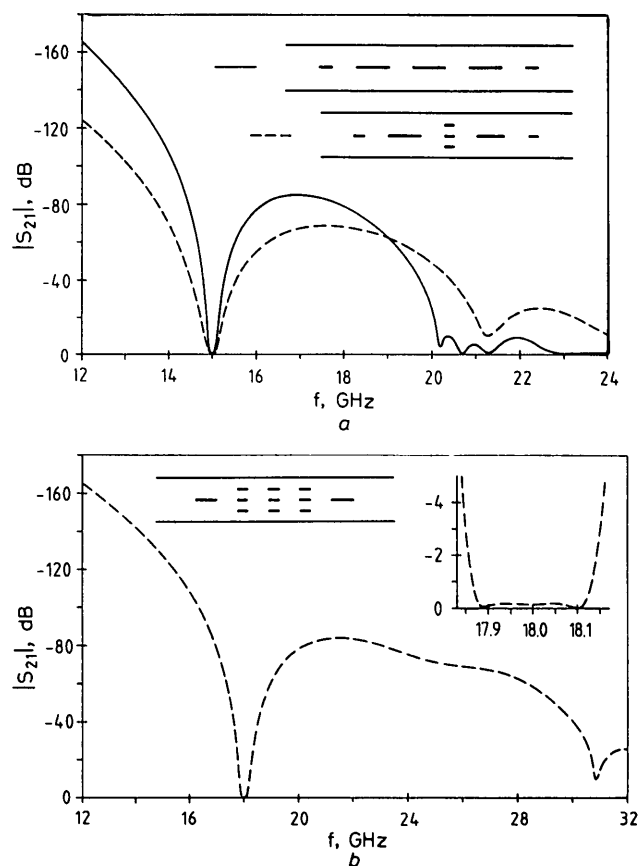


Fig. 5 Insertion loss as a function of frequency for four-resonator filters with single and triple inserts for a Ku-band example
a Central coupling section replaced by a triplet of inserts
b Three inner coupling sections replaced by a triplet of inserts
 — single metal insert
 - - - triple metal insert

The tolerance influence of the inserts on the filter characteristic is illustrated in Fig. 6 at a three-resonator Ku-band filter. If the thickness $t = 190\ \mu\text{m}$ of all inserts is increased by $+5\ \mu\text{m}$, only a slight displacement in frequency may be perceived (Fig. 6a). A more severe influence is caused by a deviation from the optimum resonator length: a frequency deviation of the passband as well as a deterioration of the ripple behaviour is obtained by reducing the length of the second resonator by $40\ \mu\text{m}$ (Fig. 6b).

4 Conclusion

Significant improvement of the stopband behaviour of *E*-plane metal insert filters is possible by merely replacing some of the conventional single insert coupling elements along the filter structure by triplets, or quintuples of metal inserts. An optimised stopband attenuation of more than 50 dB up to about 30 GHz, or 60 GHz, respectively, may be achieved, although the passbands of the corresponding filter examples are chosen to operate at the otherwise critical upper band limit of the utilised mount (at 18 GHz for

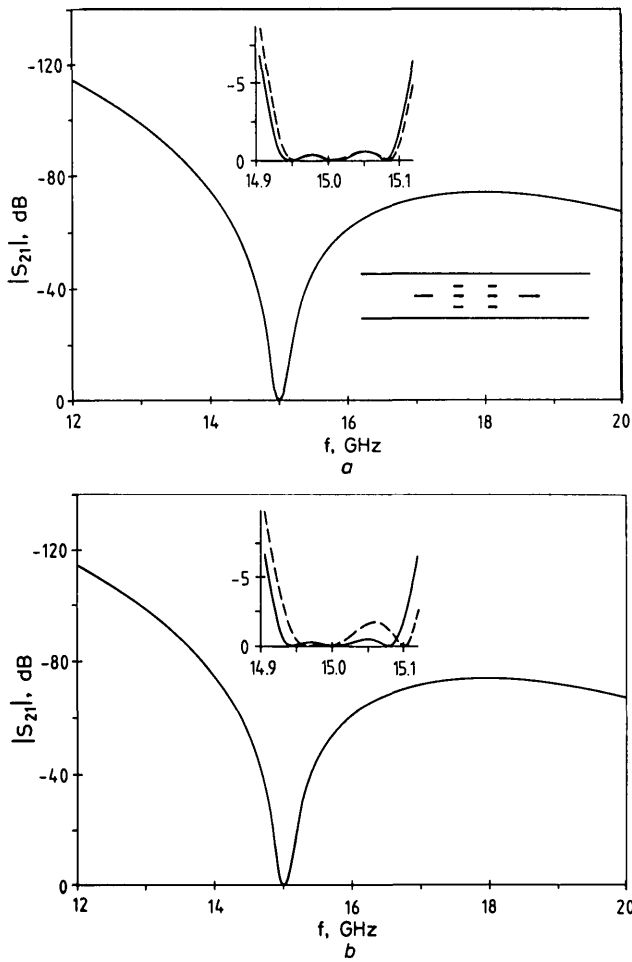


Fig. 6 Tolerance influence on the insertion loss behaviours, Ku-band filter example

a Thickness $t = 190 \mu\text{m}$ of the original inserts increased by $+5 \mu\text{m}$ (dashed-line)
b Second resonator length diminished by $40 \mu\text{m}$ (dashed-line)

Ku-band and at 40 GHz for Ka-band, respectively). As not all coupling inserts necessarily have to be replaced by multiple inserts, this improved design helps to meet the low-loss and low-cost requirements for *E*-plane filters. Moreover, the thickness of all inserts is chosen to be $t = 190 \mu\text{m}$ to make an accurate metal-etching fabrication technique possible. The computer aided design based on a rigorous field expansion allows direct mode coupling along the filter section and, therefore, the stopband behaviour to be involved in the optimisation procedure.

5 References

- KONISHI, Y., and UENAKADA, K.: 'The design of a bandpass filter with inductive strip — planar circuit mounted in waveguide', *IEEE Trans.*, 1974, **MTT-22**, pp. 869–873
- VAHLDIECK, R., BORNEMANN, J., ARNDT, F., and GRAUERHOLZ, D.: 'Optimized waveguide *E*-plane metal insert filters for millimeter-wave applications', *ibid.*, 1983, **MTT-31**, pp. 65–69
- SHIH, Y.-C., and ITOH, T.: '*E*-plane filters with finite-thickness septa', *ibid.*, 1983, **MTT-31**, pp. 1009–1013
- SHIH, Y.-C.: 'Design of waveguide *E*-plane filters with all-metal inserts', *ibid.*, 1984, **MTT-32**, pp. 695–704
- ARNDT, F., BORNEMANN, J., VAHLDIECK, R., and GRAUERHOLZ, D.: '*E*-plane integrated circuit filters with improved stopband attenuation', *ibid.*, 1984, **MTT-32**, pp. 1391–1394
- BORNEMANN, J., and ARNDT, F.: 'Metal-insert filters with improved characteristics', *IEE Proc. H, Microwaves, Opt. & Antennas*, 1986, **133**, (2), pp. 103–107
- BORNEMANN, J., and ARNDT, F.: 'Waveguide *E*-plane triple-insert filter'. Proc. 15th European Microwave Conf., Paris, France, 1985, pp. 726–731
- MARCUVITZ, N.: 'Waveguide handbook' (McGraw-Hill, 1951), chap. 5.11

- BRATHERTON, J.: 'Waveguide filters for mm wavelengths', *Microwave J.*, 1982, **25**, (7), pp. 91–95
- GRAVEN, G., and LEWIN, L.: 'Design of microwave filters with quarter-wave couplings', *Proc. IEE*, 1956, **103B**, pp. 173–175
- MATTHAEI, G.L., YOUNG, L., and JONES, E.M.T.: 'Microwave filters, impedance matching networks, and coupling structures' (McGraw-Hill, 1964), chap. 9.05
- MARIANI, E.A.: 'Designing narrow-band triple-post waveguide filters', *Microwaves*, 1965, **4**, pp. 93–97
- LI, P.G., ADAMS, A.T., LEVIATAN, Y., and PERINI, J.: 'Multiple-post inductive obstacles in rectangular waveguides', *IEEE Trans.*, 1984, **MTT-32**, pp. 365–373
- AUDA, H., and HARRINGTON, R.F.: 'Inductive posts and diaphragms of arbitrary shape and number in a rectangular waveguide', *ibid.*, 1984, **MTT-32**, pp. 606–613
- CHANG, K., and KHAN, P.J.: 'Analysis of three narrow transverse strips in waveguide'. IEEE S-MTT Inst. Microwave Symp. Dig., 1978, pp. 419–421
- CHANG, K.: 'Impedance calculation of three resonant strips on the transverse plane of a rectangular waveguide', *IEEE Trans.*, 1984, **MTT-32**, pp. 126–130
- MANSOUR, R.R., MACPHIE, R.H.: 'Scattering at an *N*-furcated parallel-plate waveguide junction', *ibid.*, 1985, **MTT-33**, pp. 830–835
- COLLIN, R.E.: 'Field theory of guided waves' (McGraw Hill, 1960), chap. 1.6, 3.4 and 5.2
- HARRINGTON, R.: 'Time-harmonic electromagnetic fields' (McGraw Hill, 1961), chap. 4–9
- ARNDT, F., BEIKE, J., GRAUERHOLZ, D., LINGEMANN, C., and BORNEMANN, J.: '*E*-plane integrated parallel-strip screen waveguide filters', *IEEE Trans.*, 1985, **MTT-33**, pp. 654–659

6 Appendix

6.1 Abbreviations in eqn. 2

$$(f^{(v)}) = (x, x, x - m_1, \dots, x - m_{i-1}, \dots, x - m_{N-1}) \quad (4)$$

$$(p^{(v)}) = (a, p_1, p_2 - m_1, \dots, p_i - m_{i-1}, \dots, a - m_{N-1}) \quad (5)$$

$$T_m^{(v)} = \frac{1}{k_{zm}^{(v)} \sqrt{\omega \mu k_{zm}^{(v)}}} \sqrt{\frac{2}{b \cdot p^{(v)}}} \quad (6)$$

$$k_{zm}^{(v)2} = \omega^2 \mu \epsilon^{(v)} - \left(\frac{m\pi}{p^{(v)}}\right)^2 \quad (7)$$

6.2 Scattering matrix elements in eqn. 3

$$(S_{11}) = (S_{22}) = -[(E) + (P) - (Q) \cdot ((E) + (P))^{-1} \cdot (Q)]^{-1} \cdot [(E) - (P) + (Q) \cdot ((E) + (P))^{-1} \cdot (Q)] \quad (8)$$

$$(S_{12}) = (S_{21}) = -[(E) + (P) - (Q) \cdot ((E) + (P))^{-1} \cdot (Q)]^{-1} \cdot [(Q) + (Q) \cdot ((E) + (P))^{-1} \cdot ((E) - (P))] \quad (9)$$

with

$$(P) = \sum_{\eta=1}^N (L^{(\eta)}) [(E) - 2((R^{(\eta)}) - (R^{(\eta)})^{-1})^{-1} \cdot (M^{(\eta)})] \cdot (M^{(\eta)}) \quad (10)$$

$$(Q) = \sum_{\eta=1}^N (L^{(\eta)}) [2((R^{(\eta)}) - (R^{(\eta)})^{-1})^{-1}] \cdot (M^{(\eta)}) \quad (11)$$

(*E*) = unity matrix

(*R*^(*n*)) = diagonal matrix of the *N*-furcated waveguide section of length l_1 (Fig. 1c) with *m* modes considered

$$\begin{pmatrix} e^{-jk_{z1} l_1} & & & 0 \\ & e^{-jk_{z2} l_1} & & \\ & & \dots & \\ 0 & & & e^{-jk_{zm} l_1} \end{pmatrix} \quad (12)$$

$(M^{(n)}) = \text{transposed matrix } (L^{(n)})'$

$(L^{(n)}) = \text{matrix containing the coupling integrals with the elements}$

$$L_{ij}^{(n)} = H_{ij}^{(n)} \frac{2}{\sqrt{a(p_\eta - m_{\eta-1})}} \sqrt{\frac{k_{zi}^{(I)}}{k_{zj}^{(II)}}} \quad (13)$$

$$H_{ij}^{(n)} = \int_{m_{\eta-1}}^{p_\eta} \left(\sin \frac{i\pi}{a} x \right) \cdot \left(\sin \frac{j\pi}{p_\eta - m_{\eta-1}} (x - m_{\eta-1}) \right) dx \quad (14)$$

Erratum

ADENIRAN, S.A.: 'A new technique for absolute temperature compensation of tunable resonant cavities', *IEE Proc. H, Microwaves, Antennas & Propag.*, 1985, **132**, (7), pp. 471-473 and 1986, **133**, (1), p. 42

Eqn. 1 should read

$$R_0 = aG_0 + \frac{2}{\pi a} \sum_{n=1}^q G_n \frac{\sin^2 n\pi a}{n^2 \pi} + \frac{2}{\pi a} \sum_{n=1}^q \frac{G_n \sin^2 n\pi a}{n\pi} a^2 \sum_{t=1}^q (-1)^t D_t$$